

On Electrostatic Positron Acceleration In The Accretion Flow Onto Neutron Stars

Roberto Turolla

*Dept. of Physics, University of Padova,
Via Marzolo 8, 35131 Padova, Italy
e-mail: turolla@astaxp.pd.infn.it*

Silvia Zane, Aldo Treves

*International School for Advanced Studies,
Via Beirut 2-4, 34014 Trieste, Italy
e-mail: zane@sissa.it, treves@astmiu.uni.mi.astro.it*

and

Andrei Illarionov

*P.N. Lebedev Physical Institute, Russian Academy of Science,
Profsoyuznaya Ul. 84/32, Moscow 117810, Russia
e-mail: illarion@dpc.asc.rssi.ru*

ABSTRACT

As first shown by Shvartsman (1970), a neutron star accreting close to the Eddington limit must acquire a positive charge in order for electrons and protons to move at the same speed. The resulting electrostatic field may contribute to accelerating positrons produced near the star surface in conjunction with the radiative force. We reconsider the balance between energy gains and losses, including inverse Compton (IC), bremsstrahlung and non-radiative scatterings. It is found that, even accounting for IC losses only, the maximum positron energy never exceeds ≈ 400 keV. The electrostatic field alone may produce energies ≈ 50 keV at most. We also show that Coulomb collisions and annihilation with accreting electrons severely limit the number of positrons that escape to infinity.

Subject headings: Acceleration of particles — Accretion, accretion disks — stars: neutron

1. Introduction

It was suggested a long time ago (Shvartsman 1970; Michel 1972; Anile, & Treves 1972; Maraschi, Reina, & Treves 1974) that accretion of a hydrogen plasma onto a neutron star must necessarily imply the presence of an electrostatic field \mathcal{E} under stationary conditions. The field \mathcal{E} arises because the radiation drag, due to the outflowing flux, acts efficiently only on electrons while practically all the mass is in protons. The electrostatic field compensates the different acceleration of the two species and allows electrons and protons to move at the same speed. Obviously \mathcal{E} is stronger the larger is the deviation from free-fall, a situation which is expected when the luminosity approaches the Eddington limit.

The typical values of the charge Q associated with the electric field are not large enough to influence the space-time around the compact object (Michel 1972), but its presence may nevertheless have interesting astrophysical consequences. Shvartsman (1970) proposed that such a system could act as an electrostatic accelerator for positrons, for which the electrostatic and radiative forces have the same direction. Balancing energy gains and losses, due mainly to inverse Compton with soft ambient photons, he estimated that positrons may be accelerated to energies of a few tens of MeV.

Although the ‘‘Shvartsman Accelerator’’ is definitely ingenious, it received little attention in the past, possibly because no obvious positron source seemed available near neutron stars. However, positrons may be generated by the radioactive decay of the neutron star crust elements subject to the bombardment of accreting particles (Reina, Tarengi, & Treves 1974; Bildsten, Shapiro, & Wasserman 1992). Pair production may be also expected in accretion models with shocks (see e.g. Shapiro, & Salpeter 1975) or in hydrostatic atmospheres kept at mildly relativistic temperatures by comptonization (Turolla, *et al.* 1994; Zane, Turolla, & Treves 1996).

Here we reconsider Shvartsman’s idea, examining the role of cooling processes different from inverse Compton (bremsstrahlung, non-radiative scattering) and the possibility that accelerated positrons survive annihilation with atmospheric electrons, escaping to infinity.

2. The Electric Field

Let us consider spherical accretion onto a neutron star ($M = 1.4M_\odot$, $R_* = 10^6$ cm) and for simplicity suppose that the accreting material is ionized hydrogen. Neglecting general relativistic corrections, the emerging luminosity is related to the accretion rate by

$$L = \frac{GM\dot{M}}{R_*}. \quad (1)$$

When L approaches the Eddington limit $L_E = 4\pi GMm_p c/\sigma_T$, the flow dynamics is strongly affected by the radiative force (see e.g. Maraschi, Reina, & Treves 1974, 1978; Miller 1990; Park & Miller 1991; Zampieri, Turolla, & Treves 1993, hereafter ZTT). Owing to the reduced effective gravity, the flow deviates from free-fall and, for $L \sim L_E$, a settling behaviour appears close to the star surface, where the velocity decreases with radius. Even a small deviation from free-fall, which is always present for a non-vanishing luminosity, implies that electrons and protons are subject to different accelerations so that an electrostatic field \mathcal{E} is built up around the star (Shvartsman 1970; Zeldovich, & Novikov 1971; Michel 1972). Although, in principle, the same argument applies to spherical accretion onto a black hole, the efficiency is so low ($\lesssim 10^{-4}$ in absence of magnetic fields, see e.g. Nobili, Turolla, & Zampieri 1991) that departures from free-fall are really negligible for any reasonable value of the accretion rate. The expression for \mathcal{E} can be easily derived considering the forces acting on the two species (e , p)

$$F_e = -\frac{L_{co}\sigma_T}{4\pi cr^2} + \frac{GMm_e}{r^2} + \mathcal{E}e \quad (2)$$

and

$$F_p = \frac{GMm_p}{r^2} - \mathcal{E}e, \quad (3)$$

where L_{co} denotes the luminosity in the frame comoving with the accretion flow. Equating the two accelerations we get

$$\mathcal{E} \simeq \frac{L_{co}\sigma_T}{4\pi cer^2} \simeq 200 \left(\frac{10^6}{r}\right)^2 \frac{L_{co}}{L_E} \text{ V/cm}. \quad (4)$$

At large radii, where $L_{co} \sim L$, the previous expression coincides with the result obtained by Maraschi, Reina, & Treves (1974, 1978) analyzing the flow equations for the two species

$$\mathcal{E} = \frac{L\sigma_T}{4\pi cer^2} \exp\left(-\frac{L}{L_E} \frac{R_*}{r}\right). \quad (5)$$

An estimate of the largest potential difference can be easily obtained integrating equation (4) assuming $L_{co} \sim L = L_E$

$$(\Delta V)_{max} \sim \frac{GMm_p}{eR_*} \simeq 200 \text{ MV} \quad (6)$$

which shows that, in principle, extremely relativistic positrons may be expected to reach infinity.

3. Compton Scattering

Here we consider a scenario in which the number density of e^+ is not zero at some radius r_{in} . Positrons are immediately accelerated by the electric field and gain energy at a rate

$$\dot{E}_{\mathcal{E}} = v e \mathcal{E}, \quad (7)$$

where v is the particle velocity. At the same time, positrons are accelerated by the radiative force and suffer radiative losses through inverse Compton (IC) scatterings with the radiation bath; $e^+ - p$ and $e^+ - e^-$ bremsstrahlung; non-radiative scatterings with the flow electrons. In this section we concentrate on IC losses, which is the only cooling process taken into account by Shvartsman, and we show that, even in this simple case, ultra-relativistic energies are not expected to be reached. In the next section we will verify that bremsstrahlung losses are negligible, but that elastic scatterings may be very efficient in transferring energy to ambient electrons and will ultimately stop the positron flow.

The energy lost by a positron for IC scattering with a radiation field of energy density U and radiation pressure K is

$$\dot{E}_{IC} = -c\sigma_T\gamma^2\beta^2(U + K), \quad (8)$$

while the gain due to the radiative force is

$$\dot{E}_{rad} = c\sigma_T\gamma^2\beta(1 + \beta^2)F, \quad (9)$$

where F is the total flux divided by c (Gurevich, & Rumyantsev 1965, all the radiation moments are here evaluated in the lab-frame). For an isotropic radiation field, $F = 0$, $K = U/3$ and the expression for the net power reduces to $\dot{E}_{IC} = -4c\sigma_T U \gamma^2 \beta^2 / 3$ (see e.g. Rybicki, & Lightman 1979). Accordingly, the positron energy changes with radius as

$$\frac{dE}{dr} = e\mathcal{E} + \sigma_T\gamma^2(1 + \beta^2)F - \sigma_T(U + K)\gamma^2\beta. \quad (10)$$

Introducing the dimensionless quantities $x = r/r_g$, $u = 4\pi r_g^2 c U / L_E$, $k = 4\pi r_g^2 c K / L_E$, and $l = L / L_E$, where r_g is the Schwarzschild radius, equation (10) can be written as

$$\frac{d\gamma}{dx} = \frac{m_p}{2m_e} \frac{1}{x^2} [l_{co} + (2\gamma^2 - 1)l - x^2(u + k)\gamma\sqrt{\gamma^2 - 1}]. \quad (11)$$

Whenever $x \ll x_c = m_p/2m_e$ the solution of equation (11) relaxes immediately to the reduced solution

$$\beta = \frac{x^2(u + k)}{2(l_{co} - l)} \left[\sqrt{1 + \frac{4(l_{co}^2 - l^2)}{x^4(u + k)^2}} - 1 \right] \quad (12)$$

irrespective of the initial particle energy. If no other processes prevent positrons from escaping (see the discussion in section 4), the terminal Lorentz factor can be obtained integrating numerically equation (11) once the radiation field in the accreting medium is known. In section 5 numerical results based on the accretion model described in ZTT will be presented.

Equation (12) also allows a close comparison between our result and Shvartsman's one. The contribution of electrostatic acceleration can be easily obtained dropping \dot{E}_{rad} in equation (10) which is, formally, equivalent to put $l = 0$ in equation (12). An upper limit for the terminal Lorentz factor in this case is given by $\gamma_{\infty}^2 = (1 + \sqrt{2})/2 \simeq 1.2$, which corresponds to a kinetic energy ~ 50 keV. This is much less than the value of tens of MeV proposed by Shvartsman. The point in Shvartsman's original analysis that should be reconsidered is the calculation of the IC losses, which were estimated in a very crude way by multiplying the energy exchange in each collision times an "optical depth" parameter, τ_+ . Even assuming that the total number of collisions suffered by the positron in traveling a radial distance r , N , is indeed related to Shvartsman's equation (2) (and this is questionable), N should be $\approx \tau_+^2$, since $\tau_+ \gg 1$. This implies that Shvartsman's Compton cooling is underestimated by a factor $\approx \tau_+ \sim 10^5$. Moreover the final particle energy is evaluated assuming that no losses are present for $\tau_+ < 1$ which results in a even larger underestimate of IC cooling.

4. Other Interactions and Relevant Timescales

In the previous section we have derived the energy equation for positrons, including only IC cooling. In

section 5 we show that, even under this favourable assumption, the positrons terminal Lorentz factor is $\lesssim 2$ (see table 1). In order to establish if indeed these mildly relativistic particles may reach infinity, we need a more thorough understanding of the physical conditions in the flow close to the star surface. In our scenario four different kinds of particles are present: “primary” electrons and protons of the accreting material, with the same number density n and temperature T , together with positrons and electrons, with number density n_+ and temperature T_+ , that are created in the atmosphere by photon–photon or particle collisions. We will limit our discussion to the case in which $z = n_+/n \ll 1$, so the number density of electrons is $n_- = n + n_+ \sim n$. The first issue that should be addressed concerns the probability that positrons annihilate with ambient electrons. This question arises quite naturally since, at variance with Shvartsman’s scenario in which highly relativistic energies are expected, now the particle energy is not high enough to ensure that the cross section for pair annihilation becomes negligible.

In the non–relativistic limit, the annihilation rate for positrons and electrons with arbitrary distribution functions is (Svensson 1982)

$$\dot{n}_+ = n_+ n_- c \pi r_e^2. \quad (13)$$

We introduce a characteristic time t_A for annihilation defined as

$$t_A = \frac{n_+}{\dot{n}_+} = \frac{1}{n_- c \pi r_e^2} \sim 1.34 \times 10^{-3} \left(\frac{10^{17}}{n} \right) \text{ s}. \quad (14)$$

Since t_A depends on n , it gives the probability of annihilation on a scale of order the density lengthscale in the accretion flow, $h \sim r$. On the other hand, a positron of energy γ covers a distance h in a time t_d

$$t_d = \int_r^{r+h} \frac{\gamma}{c \sqrt{\gamma^2 - 1}} dr \simeq \frac{\gamma}{c \sqrt{\gamma^2 - 1}} \Big|_{r+h/2} h, \quad (15)$$

and the particle survives annihilation if $t_d < t_A$. A numerical comparison between these two timescales will be given in the next section for different values of both the emergent luminosity and r_{in} . Here we only note that, in the more favourable situations in which particles are immediately accelerated up to $\gamma \sim 1.7$, this condition is met if

$$n < \frac{1}{\pi r_e^2} \frac{\sqrt{\gamma^2 - 1}}{\gamma r} \simeq 3.2 \times 10^{18} \left(\frac{10^6}{r} \right) \text{ cm}^{-3}. \quad (16)$$

This limit is fairly easy to satisfy for near Eddington accretion since $n = \dot{M}/(4\pi r^2 m_p v) \sim L_E/(4\pi r^2 m_p c^3) \approx 10^{17} (10^6/r)^2 \text{ cm}^{-3}$ close to the star surface.

Other cooling mechanisms that could influence the maximum positron energy are radiative and non–radiative scattering with ions and electrons in the accretion flow. The positron–ion bremsstrahlung energy loss is given by

$$\dot{E}_B \simeq -10^{-26} Z^2 n c E \text{ erg s}^{-1}, \quad (17)$$

where Z is the charge of the ions. This process acts on a characteristic timescale

$$t_B = \frac{E}{\dot{E}_B} \simeq 3.3 \times 10^{-2} Z^{-2} \left(\frac{10^{17}}{n} \right) \text{ s}, \quad (18)$$

which, compared with t_A , yields

$$\frac{t_A}{t_B} \simeq 4 \times 10^{-2} Z^2, \quad (19)$$

so, for pure hydrogen, bremsstrahlung losses are negligible for particles surviving annihilation and free–free could represent a competitive cooling process only for large Z .

On the other hand, the energy exchange due to collisions is indeed important and can modify substantially the picture outlined up to now. Let us introduce the energy loss rate ν_E for a test particle in a plasma of protons and electrons as

$$\dot{E}_{el} = -\nu_E E, \quad (20)$$

and focus on the non–relativistic regime. The more efficient process is radiationless, elastic scattering between positrons and electrons; positron–proton equipartition needs a larger timescale by a factor m_p/m_e . The energy loss rate can be obtained from the expression of diffusion coefficients, which, in the limit v much larger than the proton velocity, yields (see e.g. Rosenbluth, & Sagdeev 1983)

$$\nu_E \sim \frac{8\pi e^4 n \ln \Lambda}{m_e^2 v^3} \left[\frac{m_e}{m_p} + \text{erf} \left(\frac{v}{v_e} \right) - \frac{4}{\sqrt{\pi}} \frac{v}{v_e} e^{-(v/v_e)^2} \right], \quad (21)$$

where $\ln \Lambda$ is the Coulomb logarithm and v_e the electron velocity. The rate ν_E is not necessarily positive since a fast particle tends to lose energy to the plasma and a slow one to gain energy. Initial differences in the

mean velocities of positrons and electrons are eliminated by collisions in a time $t_{coll} \sim |\nu_E|^{-1}$. The importance of collisions can be quantified comparing t_{coll} with the dynamical timescale given by expression (15).

5. Numerical Estimates

In order to investigate the effects of electrostatic plus radiative acceleration on particles injected in different atmospheric layers, we have solved equation (11) varying both the accretion luminosity and the injection radius r_{in} . The run of the flow variables has been taken from the one-fluid models computed by ZTT for near-Eddington accretion of a “cold”, pure scattering medium onto neutron stars. The solutions are plotted, together with the reduced solution (equation 12), in figures 1a, b, c for $L/L_E = 0.3, 0.6$ and 0.9 , respectively. For any given luminosity, we have considered three different values of r_{in} , which correspond to a scattering optical depth $\tau \sim 0.1, 1, 5$ (see table 1), with the exception of the case $L/L_E = 0.3$, for which the maximum optical depth is $\tau \simeq 1.5$ at the star surface. This simple choice allows us to mimic the acceleration of positrons initially created in different atmospheric layers, and, increasing the luminosity, to visualize the process in the presence of more and more expanded atmospheres. In order to account for the anisotropy of the radiation field, we introduced the closure $f(\tau) = K/U$, adopting for f the same expression used by ZTT, $f(\tau) = 2/[3(1 + \tau^2)] + 1/3$. The final energies in all the cases we considered are listed in table 1. Figures 2a, b, c show the comparison between t_d and t_A for the same choice of the parameters. As can be seen from the figures, the reduced solution is always attained at small radii, but at the same time annihilation acts efficiently in the inner dense atmospheric layers preventing positrons created in optically thick regions from escaping. The chance to surviving annihilation increases for particles created in photospheric regions and above, although positrons starting at $\tau \lesssim 1$ reach infinity with a lower Lorentz factor. The larger terminal velocities are expected for low values of L when the photosphere is closer to the star surface.

Figures 3a, b, c show t_d together with t_{coll} for two different values of the gas temperature, since the efficiency of Coulomb collisions strongly depends on the difference between the test particle and the electron velocities. We note that only for $kT \gtrsim 70$ keV is

ν_e negative in an extended region near r_{in} , so the possibility that positrons gain additional energy owing to collisions appears remote. On the other hand, under the more realistic assumption that $kT \lesssim 10$ keV, as expected in typical X-ray sources, we find that mildly relativistic positrons are “de facto” prevented from reaching infinity, all differences between the mean energies of the two species being washed out by the collective effect of soft collisions.

6. Discussion

In this paper we have reconsidered acceleration of positrons near a neutron star accreting close to the Eddington limit. The radiative force and the electrostatic thrust due to the non-vanishing electric field around the neutron star are opposed by inverse Compton losses and elastic scattering with electrons of the accreting material. Ultimately, these are the main agents responsible for both the acceleration and deceleration of positrons.

The maximum energy which can be achieved by positrons owing to the electrostatic acceleration alone is limited to ~ 50 keV which differs substantially from Shvartsman’s estimate of few tens of MeV. The main contribution to the particle’s acceleration is therefore provided by the radiative force, which acts equally on electrons and positrons. We have also shown that the largest terminal Lorentz factors are still $\lesssim 2$, even if this additional gain is accounted for. A first consequence is that the maximum energies attained by positrons are in a range where pair annihilation is still important, at least for particles created at $\tau > 1$. Moreover, elastic scatterings with cold electrons in the accretion flow oppose the particle acceleration and provide an additional source of trapping. This suggests that only a fraction of positrons will actually leave the star, while the rest should annihilate and eventually contribute to a narrow 511 keV line.

Furthermore, no multiplication through electromagnetic showers either on the accreting material or on the photons can be expected, so the positron production depends mainly on the injection process. Moreover, we note that the same conclusions discussed above can be applied to particles injected below $\sim 400R_*$ (i.e. below x_c), quite independently of the initial conditions. If the source is close to the Eddington limit, even if positrons are injected with energies \sim MeV, like in radioactive decay, because of the efficiency of IC losses, their final energy will be

limited to ~ 400 keV and the possibility of outstream or annihilation will not change.

TABLE 1

THE RADIUS, THE PROTON NUMBER DENSITY AND TERMINAL KINETIC ENERGY FOR DIFFERENT VALUES OF THE ACCRETION LUMINOSITY AND OF THE SCATTERING OPTICAL DEPTH AT THE INJECTION POINT

L/L_E	τ	r_{in} 10^6 cm	$n(r_{in})$ 10^{17} cm $^{-3}$	E_∞ keV
0.3	1.5	1	19	358
0.3	1.	2	5	358
0.3	0.1	141	0.006	296
0.6	5.	1.5	61	293
0.6	1.	13	0.5	293
0.6	0.1	855	0.002	151
0.9	5.	11	5	198
0.9	1.	123	0.06	198
0.9	0.1	5000	0.0002	50

REFERENCES

- Anile, A.M., & Treves, A. 1972, Ap&SS, 19, 411
- Bildsten, L., Salpeter, E.E., & Wasserman, I. 1992, ApJ, 384, 143
- Gurevich, L.È, & Romyantsev, A.A. 1965, Sov. Physics–JETP, 20, 1233
- Maraschi, L., Reina, C., & Treves, A. 1974, A&A, 35, 389
- Maraschi, L., Reina, C., & Treves, A. 1978, A&A, 66, 99
- Michel, F.C. 1972, Ap&SS, 15, 153
- Miller, G.S. 1990, ApJ, 356, 572
- Nobili, L., Turolla, R., & Zampieri, L. 1991, ApJ, 383, 250
- Park, M.–G., & Miller, G.S., 1991, ApJ, 371, 708
- Reina, C., Treves, A., & Tarengi, M. 1974, A&A, 32, 317
- Rosenbluth, M.N., & Sagdeev, R.Z., 1983, Handbook of Plasma Physics, vol. 1, (Amsterdam: North–Holland)
- Rybicki, G.B., & Lightman, A.P., 1979, Radiative Processes in Astrophysics, (New York: Wiley)
- Shapiro, S.L., & Salpeter, E.E. 1975, ApJ, 198, 671
- Shvartsman, V.F. 1970, Astrofizika, 6, 309
- Svensson, R. 1982, ApJ, 258, 335
- Turolla, R., Zampieri, L., Colpi, M., & Treves, A. 1994, ApJ, 426, L35
- Zampieri, L., Turolla, R., & Treves, A. 1993, ApJ, 419, 311 (ZTT)
- Zane, S., Turolla, R., & Treves, A. 1996, ApJ, submitted
- Zeldovich, Ya.B., & Novikov, I.D. 1971, Relativistic Astrophysics, vol.1, (Chicago: The University of Chicago Press)

Fig. 1.— a) The positron energy vs. radius for $L/L_E = 0.3$ and scattering depth at injection 1.5, 1, and 0.1. The reduced solution is also shown (dashed line); b) same as in figure 1a for $L/L_E = 0.6$ and $\tau = 5, 1$ and 0.1; c) same as in figure 1b for $L/L_E = 0.9$.

Fig. 2.— The annihilation time t_A (dashed line) and the dynamical time t_d (solid lines) for the same values of the luminosity and injection depth as in figure 1.

Fig. 3.— The collisional time t_{coll} for $kT = 10, 70$ keV (dashed lines) and the dynamical time t_d (solid line) for $L/L_E = 0.3$ and $\tau = 1$; b) same as in figure 3a for $L/L_E = 0.6$; c) same as in figure 3a for $L/L_E = 0.9$.

Figure 1a

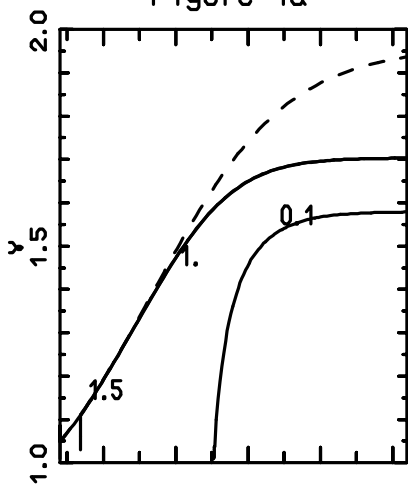


Figure 1b

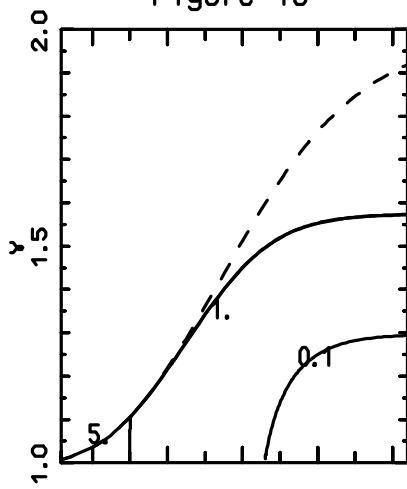


Figure 1c

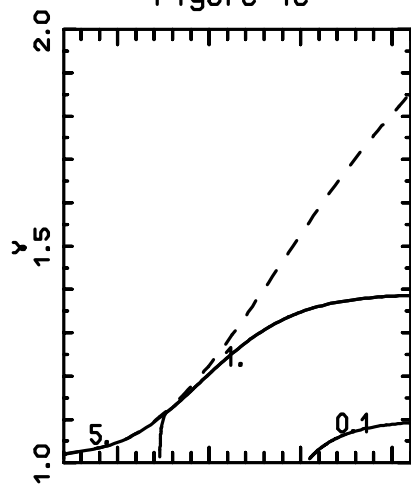


Figure 2a

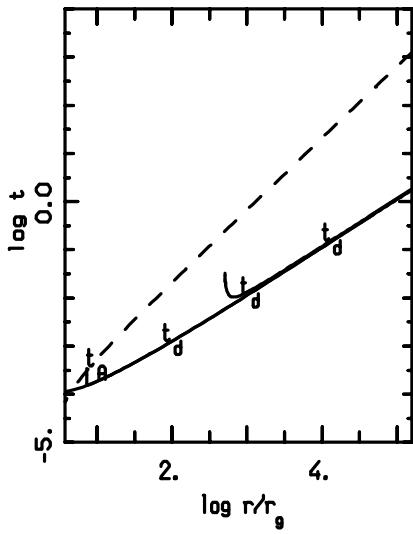


Figure 2b

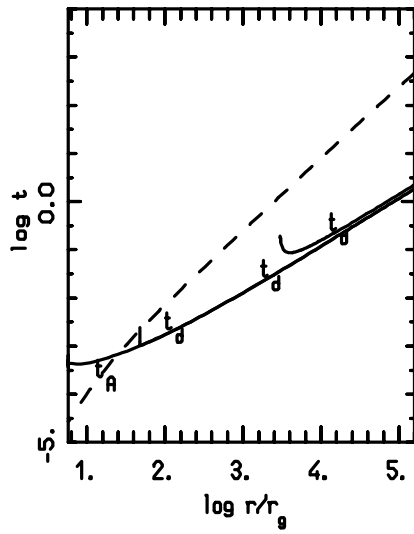


Figure 2c

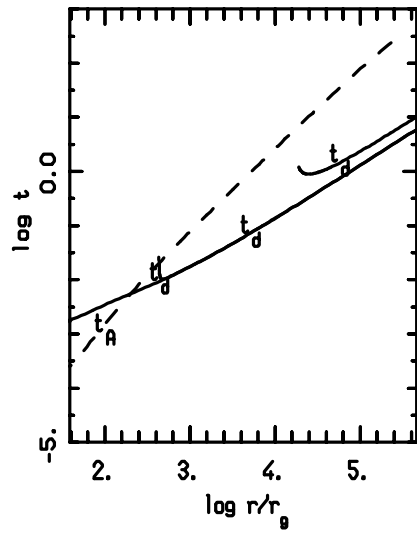


Figure 3a

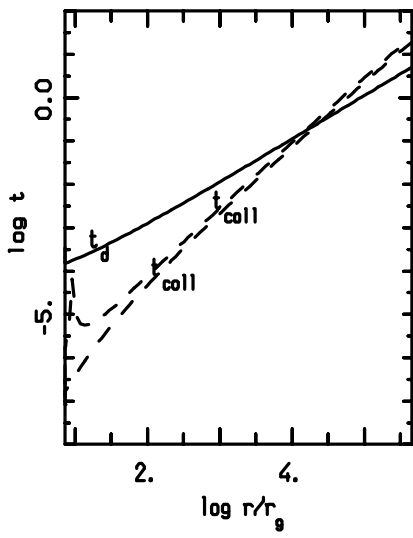


Figure 3b

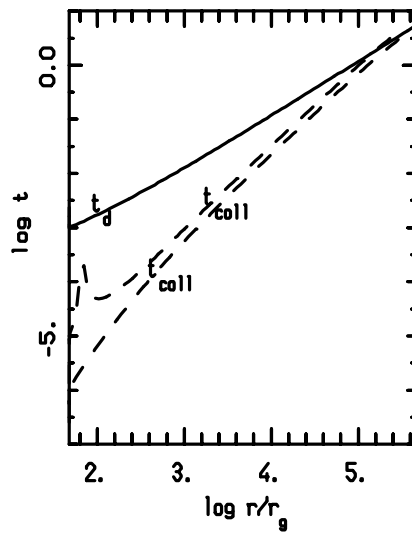


Figure 3c

